ARL-TR-10221 ● Oct 2025

# Near-Surface Disorder in Single-Crystal Silicon Carbide (4H-SiC) Induced by MeV Light Ion Irradiation

by John Derek Demaree, Noel Guardala, Zois Tsinas, and Mohamad Al-Sheikhly

## NOTICES

### Disclaimers

The findings in this report are not to be construed as an official Department of the Army position unless so designated by other authorized documents.

Citation of manufacturer's or trade names does not constitute an official endorsement or approval of the use thereof.

Destroy this report when it is no longer needed. Do not return it to the originator.

ARL-TR-10221 ● OCT 2025


# Near-Surface Disorder in Single-Crystal Silicon Carbide (4H-SiC) Induced by MeV Light Ion Irradiation

**John Derek Demaree**
*DEVCOM Army Research Laboratory*

**Noel Guardala**
*The George Washington University*

**Zois Tsinas**
*National Institute of Standards and Technology*

**Mohamad Al-Sheikhly**
*University of Maryland, College Park*

# REPORT DOCUMENTATION PAGE

| 1. REPORT DATE | 2. REPORT TYPE | 3. DATES COVERED | |
|---|---|---|---|
| | | START DATE | END DATE |
| October 2025 | Technical Report | 1 March 2018 | 1 September 2025 |

**4. TITLE AND SUBTITLE**
Near-Surface Disorder in Single-Crystal Silicon Carbide (4H-SiC) Induced by MeV Light Ion Irradiation

| 5a. CONTRACT NUMBER | 5b. GRANT NUMBER | 5c. PROGRAM ELEMENT NUMBER |
|---|---|---|
| **5d. PROJECT NUMBER** | **5e. TASK NUMBER** | **5f. WORK UNIT NUMBER** |

**6. AUTHOR(S)**
John Derek Demaree, Noel Guardala, Zois Tsinas, and Mohamad Al-Sheikhly

| 7. PERFORMING ORGANIZATION NAME(S) AND ADDRESS(ES) | 8. PERFORMING ORGANIZATION REPORT NUMBER |
|---|---|
| DEVCOM Army Research Laboratory<br>ATTN: FCDD-RLA-MF<br>Aberdeen Proving Ground, MD 21005 | ARL-TR-10221 |

| 9. SPONSORING/MONITORING AGENCY NAME(S) AND ADDRESS(ES) | 10. SPONSOR/MONITOR'S ACRONYM(S) | 11. SPONSOR/MONITOR'S REPORT NUMBER(S) |
|---|---|---|
| | | |

**12. DISTRIBUTION/AVAILABILITY STATEMENT**
DISTRIBUTION STATEMENT A. Approved for public release: distribution unlimited.

**13. SUPPLEMENTARY NOTES**
ORCIDs: John Derek Demaree, 0000-0001-8244-4761; Noel Guardala, 0000-0002-8421-1635; Zois Tsinas, 0000-0001-7712-9257; Mohamad Al-Sheikhly, 0000-0002-9666-616X

**14. ABSTRACT**
Single-crystal silicon carbide (4H-SiC) was irradiated with 1770 keV hydrogen (H) ions and 4300 keV helium (He) ions to investigate the nature of the damage that might be induced by exposure to protons, fast neutrons, or alpha particles in a nuclear reactor or waste storage environment. Raman spectroscopy and ion beam channeling were used to investigate the extent and nature of the disorder caused by light ion irradiation just under the surface of the material, rather than at the end of the ion beam range. The results suggest that the Monte Carlo simulation program SRIM correctly predicts the relative amount of ballistic displacement induced by H and He ions, as measured by the number of antisite defects and extinction of characteristic Raman features, with complete chemical disorder and elimination of important electronic properties achieved at less than 0.08 displacements per atom (dpa). In contrast, ion beam channeling measurements indicated that full structural disorder (amorphization) required much higher levels of atomic displacement. In the case of H irradiation, the rate of disorder accumulation was consistent with the direct-impact/defect-stimulated (DI/DS) model found in other studies, with no evidence of temperature-induced defect recombination. In the case of He irradiation, the overall amount of amorphization and loss of crystallinity was only 25% of that expected from the same low-temperature DI/DS model. These results are discussed in light of a possible ionization-induced recrystallization or defect recombination mechanism induced not directly by the He ions, but by ionization in the cascades of the highest energy recoil atoms.

**15. SUBJECT TERMS**
silicon carbide; ion irradiation; radiation damage; amorphization; Raman spectroscopy; ion beam channeling; Energy Sciences; Sciences of Extreme Materials; Photonics, Electronics, and Quantum Sciences

| 16. SECURITY CLASSIFICATION OF: | | | 17. LIMITATION OF ABSTRACT | 18. NUMBER OF PAGES |
|---|---|---|---|---|
| a. REPORT | b. ABSTRACT | C. THIS PAGE | | |
| UNCLASSIFIED | UNCLASSIFIED | UNCLASSIFIED | UU | 30 |

| 19a. NAME OF RESPONSIBLE PERSON | 19b. PHONE NUMBER *(Include area code)* |
|---|---|
| John Derek Demaree | (520) 691-6331 |

**STANDARD FORM 298 (REV. 5/2020)**
*Prescribed by ANSI Std. Z39.18*

## Contents

## List of Figures

## 1. Introduction

One of the key challenges for the nuclear field is the ability to develop radiation-resistant materials that can tolerate the harsh environment of intense irradiation conditions or for the long-term permanent disposal of spent nuclear fuel. In the last few decades, many experimental and theoretical efforts have been focused on a better understanding of the processes of radiation-induced damage in candidate structural materials, as well as the methods that can be used to recover the original crystallinity of the materials.[1–8] The importance of silicon carbide (SiC) has emerged from its potential nuclear[9–12] and microelectronic applications,[13–15] mainly because of its remarkable physical and chemical properties along with the low neutron absorption cross section[16] and the relatively low critical temperature for avoiding defect-induced amorphization.[17] Accordingly, this compound has received considerable attention as a coating layer in Tristructural Isotropic (TRISO) fuel particles[4,18–20] or as candidate cladding material for nuclear fuel inner canister material for long-term nuclear waste disposal.[21]

In many nuclear applications, however, SiC can be subjected to high temperature and mixed radiation fields, which may lead to the degradation of these properties. In particular, irradiation involving high linear energy transfer such as alpha particles, fast neutrons, and protons can induce significant degradation in the SiC crystal structure by reordering the Si-C covalent bonds or even destroying the crystalline structure. This atomic-scale disorder or amorphization could have a significantly deleterious effect on the performance of the material and affect its suitability for several important nuclear applications.

Following this concept, numerous studies have investigated the quality of irradiated SiC using different analytical techniques.[22] Phase transition from crystallinity to the amorphous state in SiC has been reported under the impact of hydrogen ions,[23] heavier ion beams,[24,25] or by using electrons[26,27] at a variety of temperatures. The results from these studies have demonstrated the ability of SiC to undergo damage recovery processes near room temperature—a remarkable result for such a highly bound covalent ceramic material. Other investigations have focused on understanding the mechanisms of recrystallization of irradiated SiC, such as solid phase epitaxy and ion beam induced epitaxial crystallization.[29,30] Recently, Weber et al. have investigated the ability to restore structural order through an ionization-induced healing mechanism.[3,31–33] Such a recovery mechanism could provide critical advantages for the use of SiC in nuclear reactor systems or for nuclear waste canisters.

In this study, we have attempted to understand damage accumulation near the surface region of single-crystal 4H-SiC irradiated with beams of high-energy hydrogen (H) and helium (He) ions, where surface-dominated properties such as corrosion resistance and crack initiation might be most strongly affected. The number of atomic displacements was estimated by using the SRIM-2013 Monte Carlo simulation code.[34] SRIM (Stopping and Range of Ions in Matter) tracks the interactions of individual energetic ions moving through materials to aggregate information about the extent and nature of ionization (energy transferred to target electrons) and nuclear collisions (Coulombic scattering between positively charged ions and target nuclei). Furthermore, the program tracks the interactions of both the incident ions and the subsequent interactions of recoil atoms, both of which can produce damage cascades. After many thousands of simulated ions have been followed, the program was then used to estimate the total number of atoms that should be displaced from their lattice sites for particular irradiation conditions. This simulation was used to determine the expected level of displacements for the two ion species at a variety of fluences, a number that is commonly given in displacements per atom (dpa) in order to compare ionizing species with very different defect production rates. Each irradiation condition in this study is therefore presented in this normalized format, with changes in the material cited as a function of displacements per atom, where dpa is an estimate from the SRIM program.

The irradiated SiC in this study was analyzed using Raman spectroscopy to assess the amount and nature of disorder induced by the irradiation. Raman spectroscopy is highly sensitive to SiC crystal composition and order, mainly because of the strong covalent bonds of this compound that provide an intense Raman signal, and the literature characterizing SiC polytypes and defect structures is extensive.[35-39] The irradiated areas were also analyzed using Rutherford backscattering spectrometry in a channeling geometry, a technique used to measure the overall crystallinity of a sample by assessing the reduction in elastic backscattering when a material is precisely aligned with an incident ion beam. As opposed to Raman, ion beam channeling is not generally sensitive to chemical disorder in a material like SiC, only to the lack of regular crystalline lattice structure, so it is commonly used as a measure of amorphization in irradiation studies.

## 2. Methods, Assumptions, and Procedures

Wafers of 4H-SiC (University Wafer ID 2891, <0001> orientation, laboratory quality, N doped, SSP/Si polished) were irradiated with 1770 keV protons ($H^+$ ions) and 4300 keV $He^{2+}$ ions using a 1.7 MV tandem positive ion accelerator (National Electrostatics 5SDH-2). To prepare small-area samples for Raman analysis, the

beams were focused to approximately 1 mm in diameter using a near-target electrostatic quadrupole lens. In order to prepare larger samples for ion beam channeling, and to ensure uniformity, the beam spots were focused only to 2 mm in diameter, and the targets were moved vertically and horizontally in 0.1-mm steps using a stepper motor to ensure that an area of at least 2 × 2 mm was irradiated uniformly, regardless of any inhomogeneity in the intensity of the beam across its profile. Beam currents ranged from 10 to 1000 nA on target, and the sample temperature was not controlled. For He irradiation, fluences ranged from $2.5 \times 10^{16}$ to $8.0 \times 10^{17}$ particles/cm$^2$. In the case of H irradiation, higher fluences were necessary to achieve comparable numbers of defects, and fluences ranged from $2.0 \times 10^{17}$ to $6.5 \times 10^{18}$ particles/cm$^2$.

Raman spectra were acquired in a backscattering geometry using a Horiba LabRAM spectrometer. The 633-nm solid-state laser was focused through a 150-μm spot and collected via a 50× objective lens. A 600 groove/mm grating was used, the acquisition time was set to be 3 s, and the spectra were measured from 50 to 2000 cm$^{-1}$. All the measurements were conducted at room temperature with the laser beam focused on the surface of the sample.

The crystallinity of the 4H-SiC was assessed using Rutherford backscattering spectrometry in a channeling configuration (RBS-C), using 2-MeV $He^+$ ions at a 175° backscattering angle. The samples were first axially aligned to the <0 0 0 1> axis using a five-axis goniometer near the irradiated areas to avoid additional damage accumulation during the alignment process. Elastic scattering rocking curves were then obtained using an angular scan as each previously irradiated area was placed under the aligned beam. The total scattering energy window for yield measurements was positioned at energies just below the surface peak from scattering from surface silicon atoms (1.1 MeV) and extended down to just above the scattering energy of surface carbon (0.5 MeV). It is estimated that this measurement measured the crystallinity of the samples to a depth of approximately 1 μm. The minimum yield (normalized to the randomized scattering yield) was measured for each irradiation condition and compared to that of unirradiated SiC in order to determine the degree of amorphization. In this study, “crystallinity” is defined as the ratio of the minimum yield of a sample to that of a pristine sample, and “amorphization” refers to the change in crystallinity as one moves from the as-received material (“0% amorphized,” with minimum yield equal to that of the pristine material) to complete loss of crystalline structure (“100% amorphized,” with minimum yield of 1.0).

## 3. Results and Discussion

To first estimate the impact of H and He ion beams on the material, the anticipated surface damage of the sample was evaluated by using the SRIM-2013 program code. After exposure to the ion beams, Raman spectroscopy was used to evaluate the disorder induced in the SiC in small-area irradiation samples. Finally, ion channeling was used to evaluate the crystallinity of the material in larger irradiated regions to assess the extent of amorphization.

### 3.1 Estimated Subsurface Displacement Damage Using SRIM

Energetic ions interact with matter both through ionization (energy transfer to the electrons in a material) and nuclear scattering (primarily Coulombic scattering and momentum transfer between the incident ions and positively charged nuclei). The extent of these interactions depends strongly on energy: at MeV energies, ionization is dominant, while nuclear scattering is dominant at lower energies in the keV range. Because of this effect, when materials are bombarded with ions of MeV energy, the subsurface region undergoes much more ionization than nuclear scattering, and very few target atoms receive enough direct impact energy to be moved off their lattice sites to create vacancy/interstitial pairs. As ions slow to the keV range, the chance of nuclear scattering increases dramatically, leading to much higher amounts of lattice damage at the "end-of-range" of the ion.

Just under the surface of a material, the nuclear scattering events needed to displace a Si or C atom from its lattice site are rare, but not completely absent. Especially at very high fluences, such as one might encounter in nuclear reactor or waste storage environments, the level of nuclear scattering and ion-induced disorder could be high enough to impact the long-term use of this material in radiation environments, including corrosive environments where surface defects could be important. For this reason, we chose to focus this study on the effect of light ions very near the surface of the material, rather than on end-of-range damage, which has been extensively documented using the irradiation of heavier ions.

The computer code SRIM is the most widely used Monte Carlo simulation program for predicting the range and amount of damage produced in materials subjected to ion irradiation. The program simulates the cumulative effect of thousands of individual ion tracks as they penetrate a material, scattering at low or high angles; it also follows any secondary cascades produced should one of the displaced nuclei (a recoil atom) have enough energy to produce damage tracks of its own. In this study, using MeV light ion irradiation (1770 keV $H^+$ and 4300 keV $He^{2+}$), SRIM calculates a final range of 21.4 μm for H ions and 12.4 μm for He ions. In the case of both H and He irradiation, we expect a highly disordered layer at this depth,

where the crystal structure of the SiC will be completely amorphized, even at relatively low fluences. SRIM also predicts that this layer of extremely high damage will be very narrow (0.99 μm thick for H, 0.40 μm thick for He), and the first few micrometers of material underneath the surface will be relatively undamaged. Immediately underneath the surface, SRIM predicts that the energy loss will be almost entirely due to ionization (46 eV/nm for H, and 240 eV/nm for He), with very little energy deposited via nuclear scattering (0.03 eV/nm for H, and 0.18 eV/nm for He). The ratios for electronic to nuclear stopping in this region are extremely high (1533 for H ions, and 1333 for He ions), so only a fraction of the ion energy is successful in producing a Frenkel pair, and the defect production rate is very low.

Figure 1 depicts the SRIM result for the total number of displacements expected for 1770 keV H and 4300 keV He after simulating thousands of ion impacts. Material properties for SiC used in the simulation included a density of 3.21 g/cm$^3$ and displacement energies of 35 and 20 eV, for Si and C, respectively.[40] Each of these plots was generated using a combination of two calculation methods in SRIM: "Monolayer/Surface Sputtering" and "Detailed Calculation with Full Damage Cascade" ("Monolayer" and "Full"). The Monolayer mode was used to track near-surface interactions, but it is a very slow method where ions are tracked through every layer of substrate material, using random number generators at each monolayer of material to calculate the odds of a nuclear scattering interaction. Deeper into the material, the SRIM Full mode was used, in which each individual ion is allowed to travel one unit of its mean free path in a straight line before the program pauses to calculate the odds of a scattering interaction. Using these two methods, Figure 1 shows that the amount of lattice displacement is relatively constant in the first 5 μm of the material and that 4300 keV He ions should be six to seven times more effective at creating atomic displacements than 1770 keV H ions.

This SRIM result was used to estimate the amount of displacement damage expected for the irradiation conditions used in this study and translate "fluence" into "dpa." In the case of small spot irradiations for Raman, displacements were varied from 0.01 to 0.32 dpa for both H and He ions. In the case of large-area irradiations for ion beam channeling measurements, we report on three irradiation conditions: high and low fluence samples for He ions, and a single sample for H ions. Using the fluences outlined in the experimental procedure section, the average subsurface displacement density calculated by SRIM (from Figure 1, estimated to be 2360 and 18,900 displacements/cm$^3$ for each ion/cm$^2$), and the atomic density of SiC ($4.8 \times 10^{22}$ atoms/cm$^3$), we can then report the irradiation conditions measured via ion beam channeling to be 0.06 and 0.19 dpa for the He irradiations and 0.10 dpa for H irradiation.

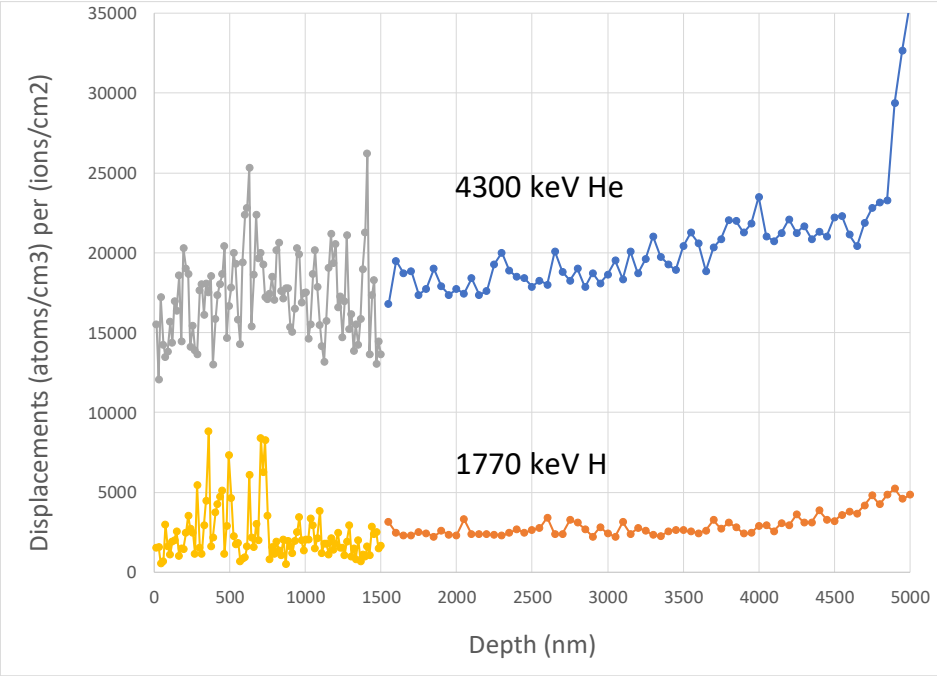


**Figure 1. SRIM calculation of displacements (dpa per unit fluence) in SiC due to irradiation by 1770 keV H ions and 4300 keV He ions. The first 1500 nm are calculated using the SRIM monolayer method and the remaining using SRIM full cascade mode. At these energies, each He ion creates six to seven times more displacements than each H ion just below the surface of the material.**

## 3.2 Raman Analysis of 4H-SiC

Raman scattering of SiC polytypes conveys structural information on the lattice dynamical vibrational properties, which allow one to establish the phonon dispersion curve for most of these polytypes.[41] Raman spectra of pristine 4H-SiC as well as material irradiated with H and He ions are discussed in more detail below.

### 3.2.1 Raman Analysis of Unirradiated 4H-SiC

First-order Raman spectra are mainly sensitive to the phonons at the center of the Brillouin zone (Γ point), with a reduced wave vector near k = 0, due to the need to conserve crystal momentum.[42] For the SiC compound, the first-order Raman spectra are polytype-dependent because of the existence of folded modes, in which phonon modes with longer wavelengths are divided into axial and planar modes. These modes are dependent on the atomic motions if they are in parallel or perpendicular directions to the c-axis, respectively.[6,36–39,43,44] Raman-active modes for pristine 4H-SiC with (0001) surface, which has a wurtzite structure and a C6υ symmetry, are represented by A1, E1, and E2 modes. Since the A1 and E1 phonon modes are both Raman and infrared active modes, they are split into longitudinal and transverse modes, and are either acoustic or optical in origin, leading to the

labels LA, TA, LO, and TO. In backscattering geometry, where the incident and collected light are parallel to the c-axis of the sample, the three essential Raman-active modes, A1, E1, and E2, are expected to be present in Raman spectra at nonresonant excitation energies.

Figure 2 shows the Raman spectrum of a pristine 4H-SiC sample, exhibiting most of the expected features reported in literature for this material. The E2(TA) peaks are noted at 195 and 203 $cm^{-1}$, although the E1(TA) is absent. A peak at 610 $cm^{-1}$ corresponds to the axial or longitudinal acoustic A1(LA) mode. The spectrum is dominated by two sharp peaks at 775 and 798 $cm^{-1}$, which correspond to the planar or transverse optical modes, E2(TO) and E1(TO) modes, respectively. The axial or longitudinal optical A1(LO) mode appears as a broad asymmetric peak at 985 $cm^{-1}$ with a full-width at half maximum value of approximately 50 $cm^{-1}$, which is slightly higher than the ideal value of 964 $cm^{-1}$ in 4H-SiC. This particular Raman mode is particularly sensitive to plasmon–phonon coupling in the material, and this shifted and broadened peak is typical of material that has been nitrogen-doped.[37,45] Second-order scattering peaks are also noted in the 1400–2000 $cm^{-1}$ region, which are due to more complex scattering interactions; these are highly sensitive to disorder and difficult to interpret, but are indicative of the highly ordered nature of the pristine material.

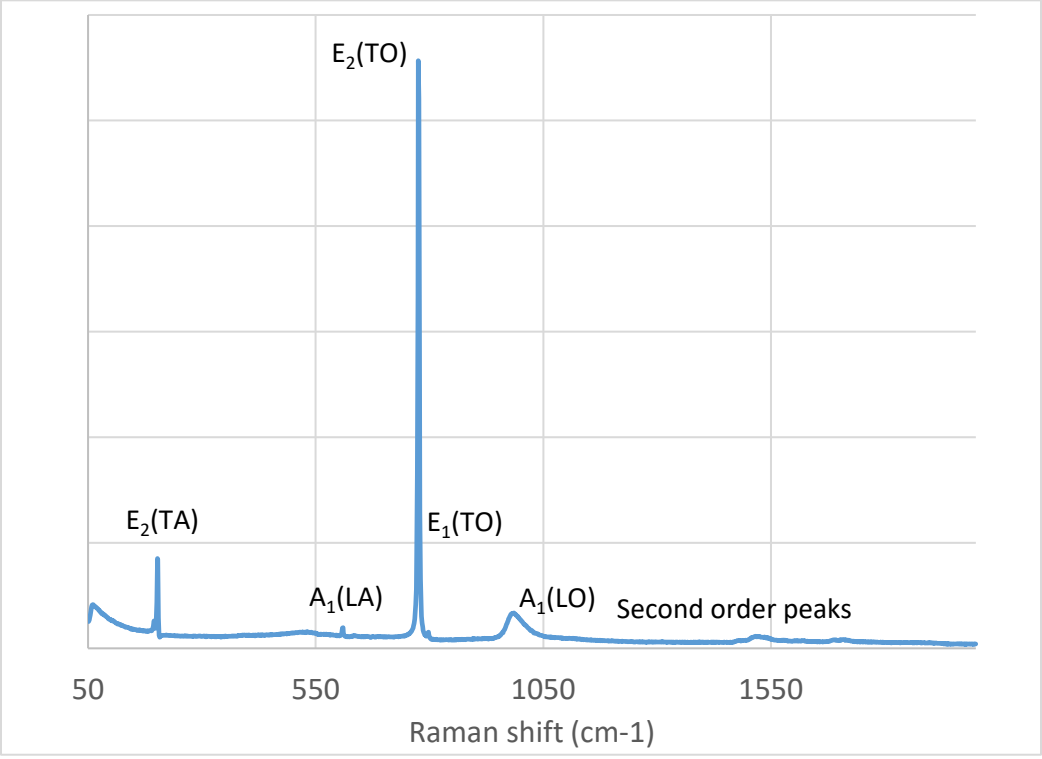


**Figure 2. Raman spectrum of pristine 4H-SiC. Peak positions are in agreement with published values, showing acoustic and optical modes dominated by the E2(TO) peak. A broad A1(LO) peak indicates a significant amount of nitrogen doping.**

### 3.2.2 Raman Analysis of Irradiated 4H-SiC

Several researchers have reported on the evolution of Raman spectra in irradiated SiC. Following the method of Sorieul et al.,[46] the resulting spectra are generally interpreted by considering three main regions: 1) Si-Si region from approximately 180 to 620 $cm^{-1}$, 2) Si-C region from 600 to approximately 1000 $cm^{-1}$, and 3) C-C region, from 1000 to 1600 $cm^{-1}$. In addition, the extinction of prominent features is used as a measure of disorder accumulation, as the introduction of vacancies, interstitial, and even antisite defects disrupts the scattering processes that lead to distinct Raman peaks.

Figure 3 shows the Raman spectra of samples irradiated with 1770 keV H ions at fluences corresponding to displacements from 0.01 to 0.32 dpa. With even the lowest amount of disorder (0.01 dpa), the Raman spectra show a complete vanishing of the acoustic branch that includes E2(TA) and A1(LA) weak modes. The region from 150 to 700 $cm^{-1}$ contains two broad peaks: the first is located between approximately 140 and 500 $cm^{-1}$ and the second slightly sharper peak is located at 600 $cm^{-1}$. The first broadband peak is characterized by possessing two sub-peaks near approximately 300 and 350 $cm^{-1}$. The second broadband peak, in the acoustic branch region, extends from 480 to 620 $cm^{-1}$ and is centered at 600 $cm^{-1}$. While it is possible that the first peak corresponds to Si-O vibrations, or even amorphous Si,[47] the second peak has been assigned by many to vibrations from distorted or disordered SiC.[48]

The most prominent part of the spectrum—the optical branch—shows a large decrease in the E2(TO) Raman peak intensity with irradiation, along with peak broadening, indicating that while those vibrations are still present in the material, the presence of defects disrupts the scattering process significantly. In addition to the general extinction of this peak, there is the complete extinction of the broad A1(LO) peak associated with nitrogen-doped SiC. In the irradiated material, a peak at 960 $cm^{-1}$ appears, which could be the A1(LO) peak of undoped material, since irradiation defects and heating could allow the nitrogen dopant to escape. There is also the development of a peak at 845 $cm^{-1}$, which has been associated with the nucleation of 6H-SiC or other stacking faults in this material,[49,50] along with a broad shelf between 850 and 960 $cm^{-1}$, which is generally associated with disordered SiC.[23] The second-order peaks noted in the pristine material have largely been extinguished, and the irradiated spectra show only broad peaks around 1130, 1190, 1460, and 1680 $cm^{-1}$, all of which could be associated with highly disordered C-C bonds, as they are in the region where Raman peaks for graphite, fullerenes, or nanocrystalline diamond are found.[51,52]

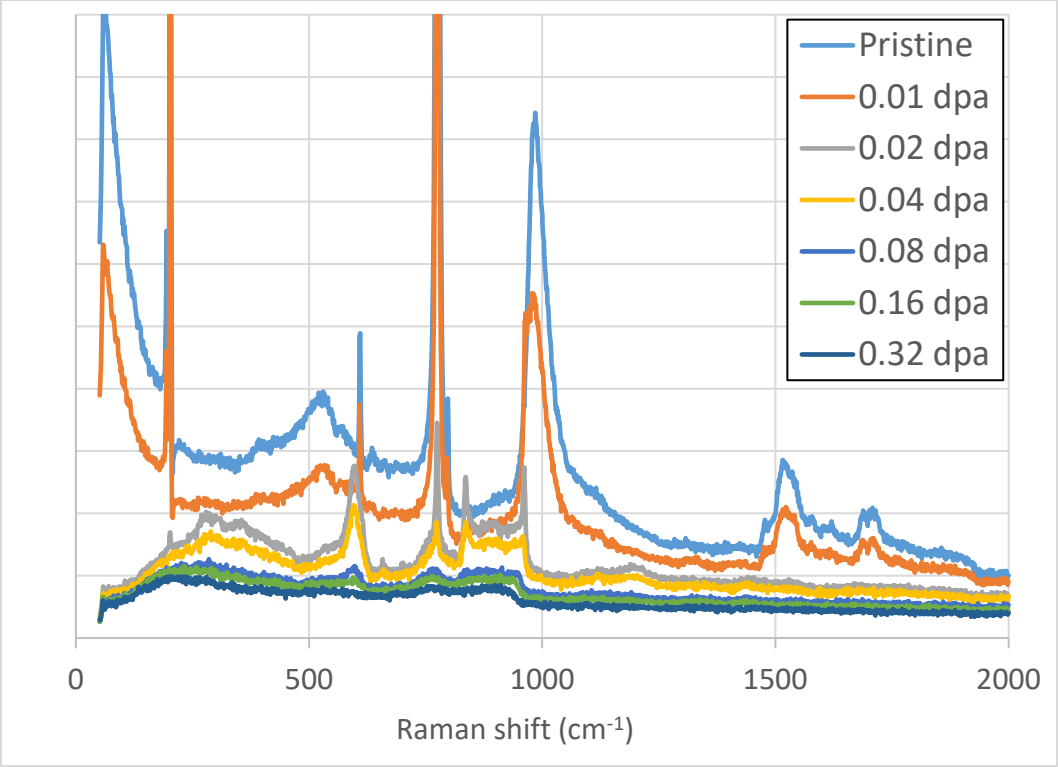


**Figure 3. Raman spectrum of 4H-SiC irradiated with 1770 keV H ions. Increasing atomic displacements (as estimated by SRIM) are correlated with extinction of the most Raman peaks, and a growth in peaks associated with Si-Si bonds, C-C bonds, and disordered SiC.**

Figure 4 shows the corresponding results for material irradiated with 4300 keV He ions at much lower fluences, but when scaled by displacements per atom, as estimated by SRIM, we find identical results. At the lowest levels of displacement, we see a reduction in all Raman peak intensity, the elimination of the second-order peaks, the vanishing or shift of the A1(LO) peak, and the development of broad features indicating disordered material. Most importantly, this indicates that the changes in the Raman spectra are independent of the ion used, and that SRIM has correctly estimated the relative efficiency of defect creation by H and He ions at these energies.

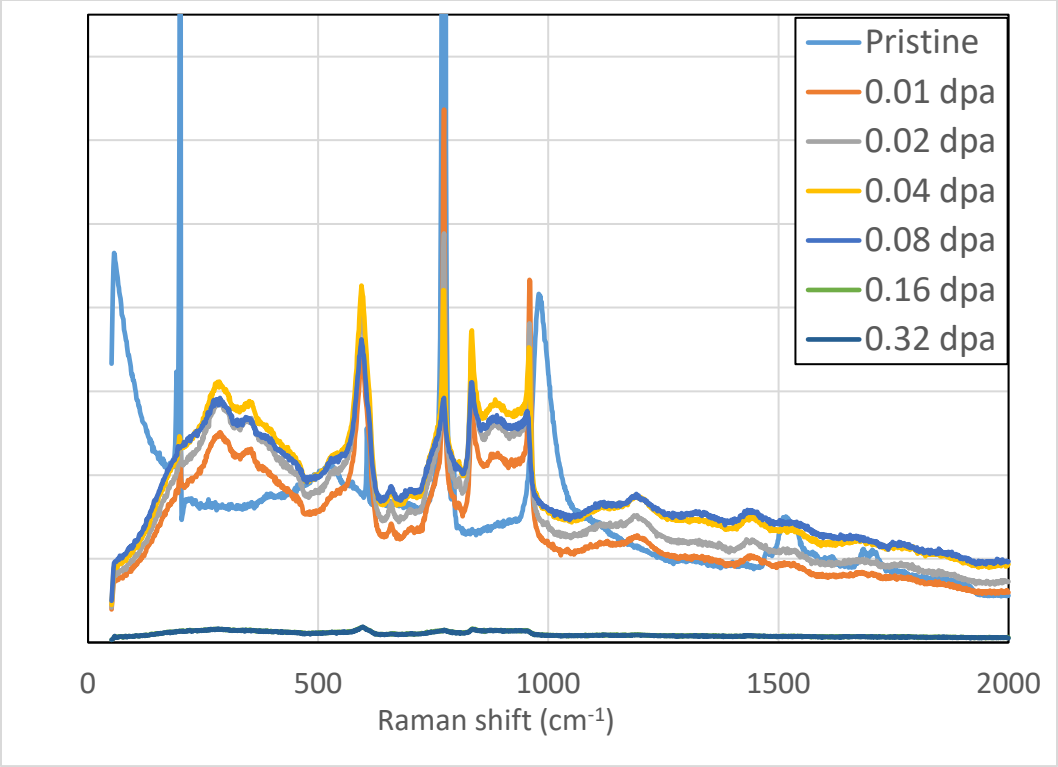


**Figure 4. Raman spectrum of 4H-SiC irradiated with 4300 keV He ions. All peaks are identical to those observed using H ions, with the same changes in chemical disorder noted.**

Following the method of Sorieul et al.,[46] the intensity of the most prominent Raman feature —the E2(TO) peak—was plotted as a function of displacements per atom, and these results are shown in Figure 5 for the spectra shown above, as well as additional spectra taken from repeated irradiation experiments. Relative disorder is here defined as the intensity of the E1(TO) peak with the pristine material plotted at zero, and the results scaled to the small intensity of the highly damaged material found after 0.32 dpa (relative disorder = 1). No difference is seen in the rate of damage accumulation with H versus He ions, and the accumulation of this disorder saturates at displacement levels as low as 0.08 dpa, which is consistent with published measurements of chemical disorder using heavy ion irradiation in this material.[46]

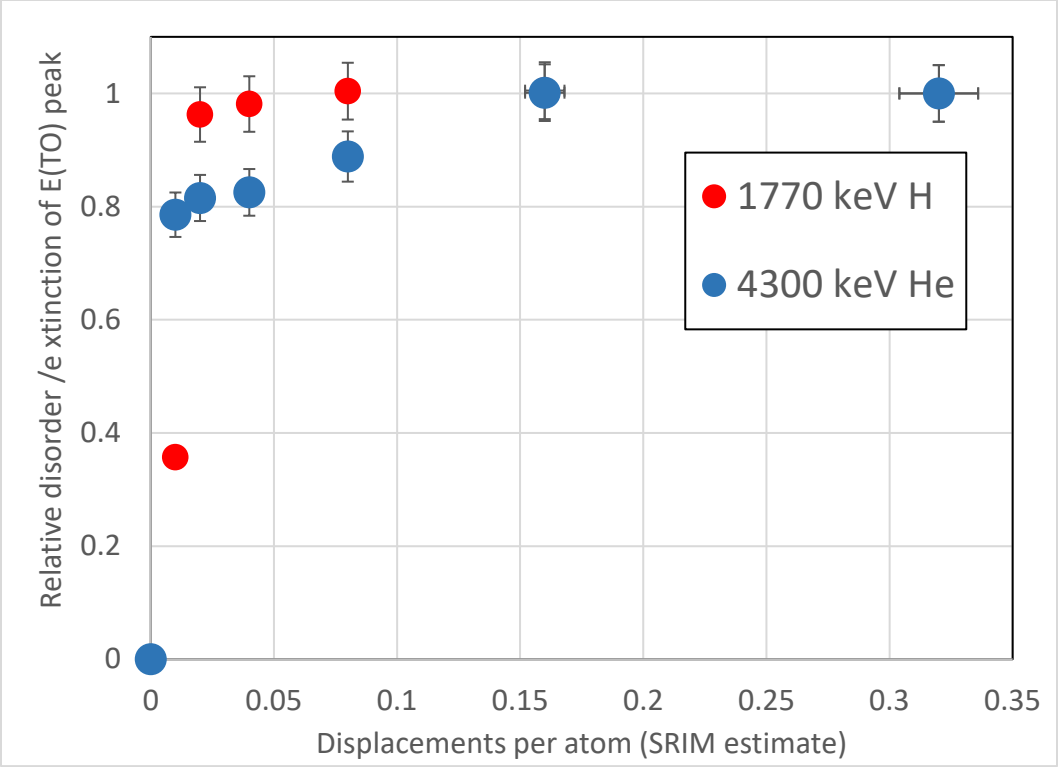


**Figure 5. Relative disorder in 4H-SiC as a function of displacement density as measured by the extinction of the E(TO) peaks. No difference is noted between H and He irradiation when scaled by dpa, indicating similar accumulation of chemical disorder in both cases.**

## 3.3 Ion Beam Channeling Measurements of 4H-SiC

Elastic scattering rocking curves from RBS-C are shown in Figure 6 for pristine SiC, and for SiC exposed to 1770 keV $H^+$ irradiation at fluences expected by SRIM estimates to produce 0.10 dpa in the near-surface region. The minimum yield of the pristine SiC was 0.05, which is typical of high-quality single-crystal material, and reflects good beam collimation and sample alignment in the RBS-C measurement system. In contrast, SiC exposed to H ion irradiation had a minimum yield of 0.22, indicating a significant degree of disorder in the first micrometer beneath the surface of the material. This change in minimum yield indicates that the subsurface SiC, exposed to 0.10 dpa via H irradiation, has been 18% amorphized.

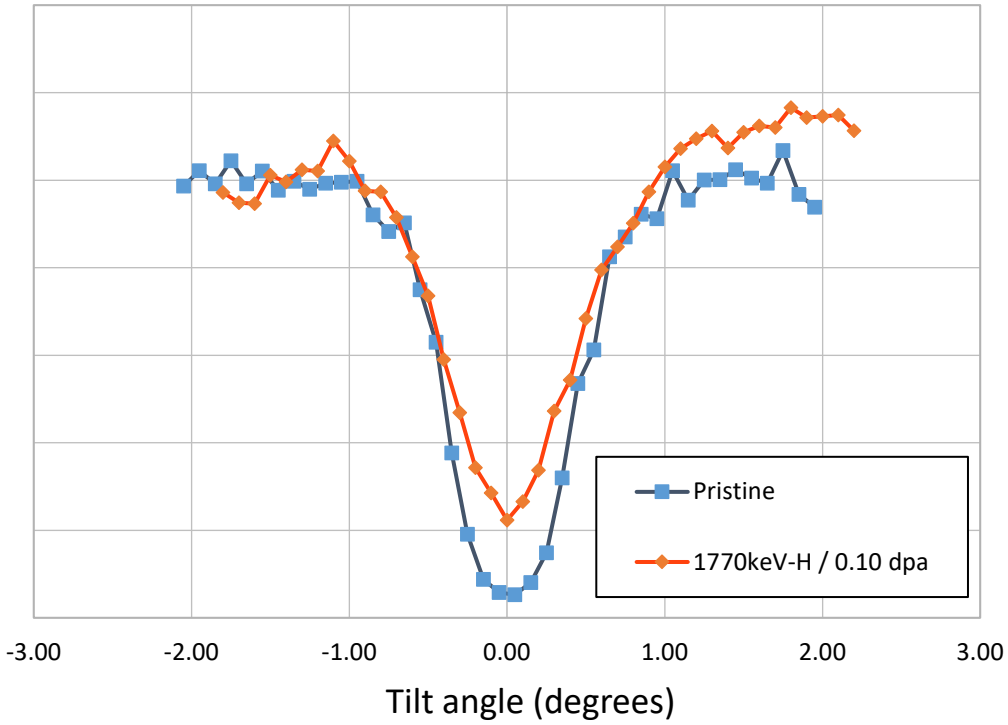


**Figure 6. Backscattering yield from angular scan across <0 0 0 1> axis of 4H-SiC before and after irradiation with 1770 keV $H^+$ ions to an estimated displacement density of 0.10 dpa.**

Figure 7 shows a similar measurement for SiC exposed to 4300 keV $He^{2+}$ beams at two fluences expected by SRIM to induce both a lower and higher number of ballistic interactions: 0.06 and 0.19 dpa. The minimum yields of this irradiated material were found to be 0.062 and 0.129, respectively, corresponding to an estimated amorphization of only 2% and 9%.

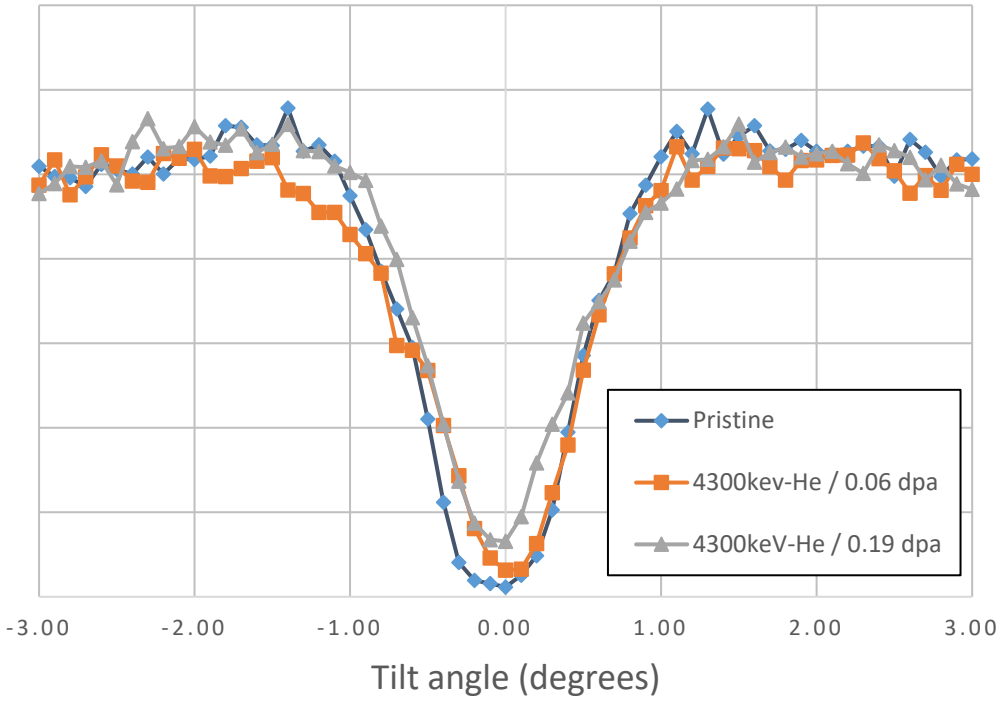


**Figure 7. Backscattering yield from an angular scan across <0 0 0 1> axis of 4H-SiC before and after irradiation with 4300 keV He ions to an estimated displacement density of 0.19 dpa.**

Past work by Weber[24,53] and others has characterized the accumulation of irradiation-induced disorder in SiC using a sigmoidal damage accumulation fit, best described using a direct-impact/defect-stimulated (DI/DS) model. Under conditions where thermal recombination of defects is possible, the defect-stimulation contribution is suppressed, and the heterogeneous accumulation of disorder toward full amorphization can be delayed. While complete amorphization of SiC can be achieved at 0.30 dpa at 170 K, irradiation temperatures of 375 K typically require 0.60 dpa, as defects are less effective at stimulating amorphization.[17] Weber found that the activation energy of defect recovery processes, which begin around 300 K, is approximately 0.23 eV, and so for temperatures exceeding a critical temperature, it may not be possible to fully amorphize the material using ion irradiation.[53,54]

Figure 8 shows a typical sigmoidal amorphization curve from one of these published studies,[55] and the three measurements reported in this study are also placed on this figure. The amorphization fraction achieved here using 1770 keV H irradiation (18%) corresponds well with these previous studies. This result is also consistent with the fact that light ion irradiation (both H and He) creates much less dense defect cascades than heavy ion irradiation, so one expects a smaller contribution from defect stimulation and a damage accumulation closer to that predicted by solely direct-impact models. The data point lies just below the 370 K

curve reported by Weber et al.,[55] indicating a possible slight thermal influence on this measurement, possibly from simple beam heating.

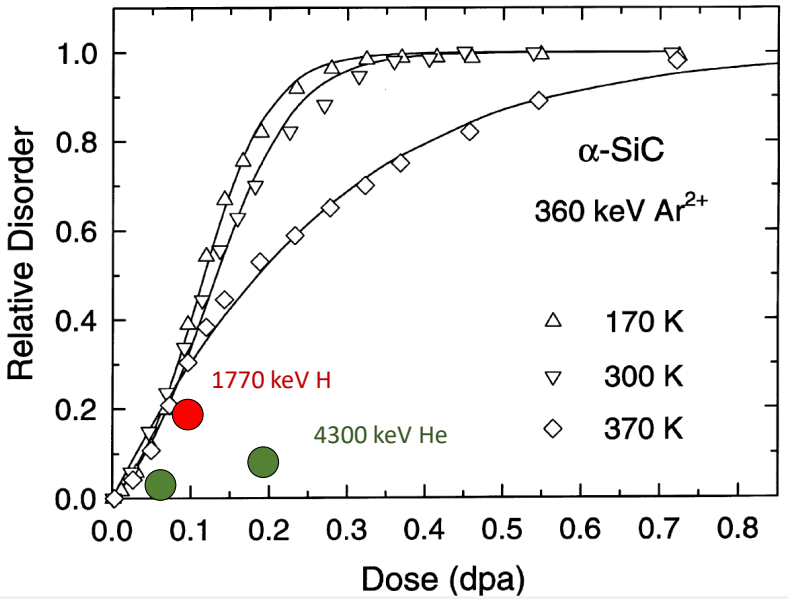


**Figure 8. Damage accumulation curves reproduced from Weber et al.[55] validating a DI/DS model using Ar ion irradiation. The three results of this study using H and He are shown in relation to this published data.**

In the case of He irradiation, one would expect similar behavior as with H irradiation, in that defects are not created in dense clusters where in-cascade recombination is likely. With similar heat loads on the sample, one expects similar irradiation temperatures in both experiments; with only minor thermally induced recombination to retard damage accumulation, we expected the amorphization fraction to scale simply with the number of defects produced (approximately six to seven times more, as estimated by SRIM).

The He irradiation results in this study, however, fall significantly below the expected curve, and much lower than that of H irradiation to a similar dpa. In fact, a significantly higher displacement value (0.19) created an amorphization fraction of only 9%, one-tenth of that expected in an athermal model, and less than one-quarter of that expected by the DI/DS model at moderate thermal conditions.

The low level of amorphization in He-irradiated SiC may be explained by considering the phenomenon of ionization-induced annealing. When the amount of energy deposited via ionization significantly exceeds that deposited into a material via defect creation, such as near the surface of SiC undergoing heavy ion bombardment, it has been reported that damage accumulation can be significantly retarded. That is, when a sufficiently high amount of energy is present in the electronic system, that energy is available to induce localized annealing of Si and

C atoms that have been ballistically displaced from their original lattice locations, returning the material to a crystalline state rather than an uncoordinated amorphous configuration. This phenomenon in SiC has been extensively studied and reported by Weber et al.[3,31,56] in a series of papers investigating the ionization density thresholds necessary to either avoid the creation of persistent defects ("in-cascade annealing") or to anneal out preexisting defects created in a prior process. Using highly ionizing beams of Ni, Si, O, and C, Zhang et al.[31] determined that at least 1400 eV/nm must be deposited via ionization before preexisting defects could be removed via annealing, while Xue et al.[3] found a slightly lower threshold (1000 eV/nm) to slow damage accumulation via in-cascade annealing.

In this study, however, the ionization density expected from H and He irradiation is significantly lower than either of these reported thresholds, so this effect was not expected to play a role in amorphization. In the case of 1770 keV H, SRIM predicts an ionization density of only 40 eV/nm at the surface, much lower than the 1000 eV/nm threshold reported in the literature. Similarly, the ionization density of 4300 keV He (240 eV/nm) is also much lower than the reported threshold. Because of these low levels of ionization, an ionization-induced annealing effect was not anticipated for either the H or He irradiation in this study.

However, one must also consider the secondary effect of ionization from highly energetic recoil atoms. It is possible that a few primary knock-on recoil atoms of Si and C near the surface—where the incoming ion has nearly its full incident energy—might themselves create a significant amount of ionization in their cascades. In the case of 1770 keV H ions, the maximum recoil energies are fairly low (235 keV for Si and 501 eV for C), capable of creating cascades with ionization densities of 700 and 1000 eV/nm, respectively. Thus, in the case of 1770 keV H, even this recoil-induced ionization density is lower than the reported thresholds for healing. However, in the case of 4300 keV He ions, some recoil atoms have much higher energies because of higher ion energy and higher momentum transfer from a heavier incident particle; recoils from 4300 keV He ions will have energies as high as 1.9 MeV (Si) and 3.2 MeV (C). These recoil atoms will deposit high amounts of ionization energy (2400 eV/nm for Si recoils, 1800 eV/nm for C recoils) in their secondary cascades, both of which exceed the reported ionization density thresholds for recombination of local defects and/or annealing of preexisting defects from earlier collisions.

It should be noted that very few recoils receive the maximum possible energy transfer from direct backscattering and would be able to create such highly ionized cascade regions. Calculations of the mean recoil energy are complicated by non-isotropic scattering considerations, and beyond the scope of this work, but a simple relativity kinematics calculation, along with ionization estimates from SRIM,

indicates that most of the recoils from 4300 keV He irradiation would exceed a 1000 eV/nm ionization density threshold, while recoils from 1770 keV H irradiation do not. This is the most likely explanation for the significant lack of amorphization in the case of 4300 keV He irradiations, and the absence of this healing mechanism in the case of 1770 keV H irradiation.

This result is consistent with the observation of Jiang et al.[57] that recombination of defects produced by He irradiation is active at anomalously low temperatures (as low as 160 K in their study), and that in the case of He ion irradiation, much higher numbers of displacements are required to produce regions of amorphization than with comparable Si ion irradiation (where the energy deposition ratio for ionization/nuclear scattering is smaller). Although it was not the purpose of their study, which concerned defect creation at the end of range for He irradiation, it is possible that the delay in amorphization noted there was a result of recoil-induced ionization providing the necessary conditions for an ionization-induced healing mechanism. Additional studies would be needed to confirm and understand this recoil-induced mechanism, perhaps using direct implantation of Si and C atoms at energies bracketing the reported 1000 eV/nm threshold, as well as lower-energy He irradiation where recoils should have insufficient energy to achieve this condition.

## 4. Conclusions

This study has identified two important and distinct regimes of near-surface damage—chemical disorder and amorphization—that occur at very different damage thresholds, quantified using a "displacement-per-atom" description.

The electronic structure of 4H-SiC was found to be highly sensitive to even the smallest number of atomic displacements from incident ion beams. As characterized using Raman spectroscopy, damage as low as 0.01 dpa reduced or eliminated several distinct features of the Raman scattering spectrum, and at levels over 0.08 dpa, nearly all features were obscured. The threshold was generally the same for both 1770 keV H ions and 4300 keV He ions, and was likely due to the accumulation of antisite defects.

Ion beam channeling was used to evaluate the crystallinity of the material in the near-surface region and found that even after the electronic properties had been degraded (dpa > 0.08), the material remained mostly crystalline. In the case of H irradiation, the extent of amorphization at a given displacement level generally agreed with published studies of SiC amorphization, but He-irradiated samples remained mostly crystalline despite damage levels as high as 0.19 dpa.

This reduced level of amorphization is consistent with the ionization-induced in-cascade healing noted by others, even though direct ionization by primary beam is below the previously published thresholds for ionization-induced healing. We speculate that the most energetic primary recoil atoms (both Si and C) may create enough ionization to heal their own damage cascades. H irradiation at these incident energies cannot activate this ionization-induced healing mechanism, as neither the primary beam nor the recoils create enough ionization to reach the threshold. Therefore, the total amorphization produced by 1770 keV H irradiation is in line with expected values for simple displacement accumulation without recombination.

The anomalously low amorphization of the material from He irradiation indicates that SiC could be extremely resistant to physical degradation from exposure to alpha-emitting radioisotopes, or neutron-rich environments in which alphas could be generated, and is therefore a promising candidate for nuclear reactor environments or nuclear waste storage, even if its susceptibility to chemical disorder and electronic degradation makes it less suitable for radioisotopic power devices.

## 5. References


1. Weber WJ et al. Radiation effects in glass used for immobilization of high-level waste and plutonium disposition. J Mater Res. 1997;12:1946–1978.
2. Tan L, Katoh Y, Snead LL. Development of castable nanostructured alloys as a new generation RAFM steels. J Nucl Mater. 2018;511:598–604.
3. Xue H, Zhang Y, Weber WJ. In-cascade ionization effects on defects production in 3C silicon carbide. Mater Res Lett. 2017;7:494–500.
4. Snead LL et al. Handbook of SiC properties for fuel performance modeling. J Nucl Mater. 2007;371:329–377.
5. Wang SX et al. Radiation stability of gadolinium zirconate: a waste form for plutonium disposition. J Mater Res. 1999;14:4470–4473.
6. Weber WJ, Navrotsky A, Stefanovsky S, Vance ER, Vernaz E. Materials science of high-level nuclear waste immobilization. MRS Bulletin. 2009;34:46–53.
7. Kim S, Szlufarska I, Morgan D. Ab initio study of point defect structures and energetics in ZrC. J Appl Phys. 2010;107:053521.
8. Shrader D et al. Ag diffusion in cubic silicon carbide. J Nucl Mater. 2011;408:257–271.
9. Diomidis N, Johnson LH, Bastid P, Allen C. Design development of a copper-coated canister for the disposal of spent fuel in a deep geological repository in Opalinus Clay. Corrosion Engineering, Science and Technology. 2017;52:31–39.
10. Katoh Y, Kohyama A, Nozawa T, Sato M. SiC/SiC composites through transient eutectic-phase route for fusion applications. J Nucl Mater. 2004;329–333:587–591.
11. Riccardi B et al. Issues and advances in $SiC_f$/SiC composites development for fusion reactors. J Nucl Mater. 2004;329–333:56–65.
12. Katoh Y, Snead LL, Szlufarska I, Weber WJ. Radiation effects in SiC for nuclear structural applications. Curr Opin Solid State Mater Sci. 2012;16:143–152.
13. Madar R. Materials science: silicon carbide in contention. Nature. 2004;430:974–975.

14. Szlufarska I, Kalia RK, Nakano A, Vashishta P. Atomistic mechanisms of amorphization during nanoindentation of SiC: a molecular dynamics study. Phys Rev B. 2005;71:174113.

15. Lee TH, Bhunia S, Mehregany M. Electromechanical computing at 500 °C with silicon carbide. Science. 2010;329:1316–1318.

16. Huang H, Choniem N. Neutron displacement damage cross section for SiC. J Nucl Mater. 1993;199:221–230.

17. Weber WJ, Wang LM. The temperature dependence of ion-beam-induced amorphization in β-SiC. Nucl Instrum Methods Phys Res, Sect B. 1995;106:298–302.

18. Hosemann P et al. Mechanical characteristics of SiC coating layer in TRISO fuel particles. J Nucl Mater. 2013;442:133–142.

19. Besmann TM et al. Modeling deep burn TRISO particle nuclear fuel. J Nucl Mater. 2012;430:181–189.

20. Tan L, Allen TR, Hunn JD, Miller JH. EBDS for microstructure and property characterization of the SiC-coating in TRISO fuel particles. J Nucl Mater. 2008;372:400–404.

21. Knorr J et al. SiC encapsulations of (V)HTR components and waste by laser beam joining of ceramics. Nucl Eng Des. 2008;238:3129–3135.

22. Zinkle SJ, Snead LL. Influence of irradiation spectrum and implanted ions on the amorphization of ceramics. Nucl Instrum Methods Phys Res, Sect B. 1996;116:92–101.

23. Huang K et al. Defect formation in MeV $H^+$ implanted GaN and 4H-SiC investigated by cross-sectional Raman spectroscopy. Nucl Instrum Methods Phys Res, Sect B. 2017;406:656–661.

24. Weber WJ, Yu N. In situ and ex situ investigation of ion-beam-induced amorphization in α-SiC. Nucl Instrum Methods Phys Res, Sect B. 1997;127/128:191–194.

25. Grimaldi MG, Calcagno L, Musumeci P, Frangis N, Van Landuyt J. Amorphization and defect recombination in ion implanted silicon carbide. J Appl Phys. 1997;81:7181–7185.

26. Inui H, Mori H, Fujita H. Electron-irradiation-induced crystalline to amorphous transition in α-SiC single crystals. Philos Mag B. 1990;61:107–124.

27. Inui H, Mori H, Suzuki A, Fujita H. Electron-irradiation-induced crystalline-to-amorphous transition in β-SiC single crystals. Philos Mag B. 1992;65:1–14.

28. McHague CJ, Williams JM. Ion implantation effects in silicon carbide. Nucl Instrum Methods Phys Res, Sect B. 1993;80/81:889–894.

29. Heera V, Stoemenos J, Kögler R, Skorupa W. Amorphization and recrystallization of 6H-SiC by ion-beam irradiation. J Appl Phys. 1995;77:2999–3009.

30. Heera V, Kögler R, Skorupa W, Stoemenos J. Complete recrystallization of amorphous silicon carbide layers by ion irradiation. Appl Phys Lett. 1995;67:1999–2001.

31. Zhang Y et al. Ionization-induced annealing of pre-existing defects in silicon carbide. Nat Commun. 2015;6:8049.

32. Weber WJ, Duffy DM, Thomé L, Zhang Y. The role of electronic energy loss in ion beam modification of materials. Curr Opin Solid State Mater Sci. 2017;21:285–298.

33. Zhang Y et al. Coupled electronic and atomic effects on defect evolution in silicon carbide under ion irradiation. Curr Opin Solid State Mater Sci. 2017;21:285–298.

34. Ziegler JF. Interactions of ions with matter; n.d. www.srim.org.

35. Feldman DW, Parker Jr JH, Choyke WJ, Patrick L. Raman scattering in 6H SiC Phys Rev. 1968;170:698–704.

36. Feldman DW, Parker Jr JH, Choyke WJ, Patrick L. Phonon dispersion curve by Raman scattering in SiC, polytypes 3C, 4H, 6H, 15R, and 21R. Phys Rev 1968;173:787–793.

37. Burton JC et al. Spatial characterization of doped SiC wafers by Raman spectroscopy. J Appl Phys. 1998;11:6268–6273.

38. Nakashima S, Hariman H. Raman investigation of SiC polytypes. Phys Stat Sol(a). 1997;162:39–64.

39. Burton JC, Sun L, Long FH, Feng ZC, Ferguson IT. First- and second-order Raman scattering from semi-insulting 4H-SiC. Phys Rev B. 1999;59:7282–7284.

40. Devanathan R, Weber WJ, Gao F. Atomic scale simulation of defect production in irradiated 3C-SiC. J Appl Physics. 2001;90:2303. https://doi.org/10.1063/1.1389523

41. Fan J, Chu PK. General properties of bulk SiC. In: Derby B, editor. Silicon carbide nanostructures: fabrication, structure, and properties. Springer; 2014. p. 7–114.

42. Dong J, Chen A-B. Fundamental properties of SiC: crystal structure, bonding energy, band structure, and lattice vibrations. In: Feng ZC, editor. SiC Power Materials. Springer, Berlin, Heidelberg; 2004. p. 63–87. (Springer series in materials science; vol. 73). https://doi.org/10.1007/978-3-662-09877-6_2

43. Hayes W, Loudon R. Scattering of light by crystals. 1st ed. Wiley; 1978.

44. Miro S, Costantini J-M, Huguet-Garcia J, Thomé L. Recrystallization of hexagonal silicon carbide after gold ion irradiation and thermal annealing. Philos Mag. 2014;94:3898–3913.

45. Bauer M. 2010: Raman spectroscopy of laser induced material alterations [Dissertation, Ludwig-Maximilians-Universität München].

46. Sorieul S, Costantini J-M, Gosmain L, Thomé L, Grob J-J. Raman spectroscopy study of heavy-ion-irradiated α-SiC. J Phys: Condens Matter. 2006;18:5235–5251.

47. Mélinon P et al. Si-C bonding in films prepared by heterofullerene deposition. Phys Rev B. 2002;65:125321–10.

48. Nakashima S, Kisoda K, Niizuma H, Harima H. Raman scattering of disordered SiC. Physica B. 1996;219 & 220:371–373.

49. Nakashima S, Mitani T, Tomobe M, Kato T, Okumura H. Raman characterization of damaged layers of 4H-SiC induced by scratching. AIP Adv. 2016;6:015207.

50. Nakashima S, Nakatake Y, Harima H, Katsuno M, Ohtani N. Detection of stacking faults in 6H-SiC by Raman scattering. Appl Phys Lett. 2000;77:3612–3614.

51. Pimenta MA et al. Studying disorder in graphite-based systems by Raman spectroscopy. Phys Chem Chem Phys. 2007;9:1276–1291.

52. Miro S, Costantini J-M, Sorieul S, Gosmain L, Thomé L. Recrystallization of amorphous ion-implanted silicon carbide after thermal annealing. Philos Mag Lett. 2012;92:633–639.

53. Weber WJ. Models and mechanisms of irradiation-induced amorphization in ceramics. Nucl Instrum Methods Phys Res, Sect B. 2000;166–167:98–106.

54. Weber WJ, Jiang W, Thevuthasan S. Defect annealing kinetics in irradiated 6H-SiC. Nucl Instrum Methods Phys Res, Sect B. 2000;166–167:410–414.

55. Weber WJ, Yu N, Wang LM, Hess NJ. Temperature and dose dependence of ion-beam-induced amorphization in α-SiC. J Nucl Materials. 1997;244:258–265.

56. Thome L et al. Radiation effects in nuclear materials: role of nuclear and electronic energy losses and their synergy. Nucl Instrum Methods Phys Res, Sect B. 2013;307:43–48.

57. Jiang W, Weber WJ, Thevuthasan S, McCready DE. Displacement energy measurements for ion-irradiated 6H-SiC. Nucl Instrum Methods Phys Res, Sect B. 1999;148:557–561.

## List of Symbols, Abbreviations, and Acronyms

| | |
|---|---|
| 4H-SiC | silicon carbide, 4H polytype |
| DI/DS | direct-impact/defect-stimulated |
| dpa | displacements per atom |
| H | hydrogen |
| He | helium |
| keV | kiloelectronvolt |
| LO | longitudinal mode |
| MeV | megaelectronvolt |
| RBS-C | Rutherford backscattering spectrometry in a channeling configuration |
| SiC | silicon carbide |
| SRIM | Stopping and Range of Ions in Matter |
| TO | transverse mode |

| | |
|---|---|
| 1 (PDF) | DEFENSE TECHNICAL INFORMATION CTR DTIC OCA |
| 1 (PDF) | DEVCOM ARL FCDD RLB CI TECH LIB |